Figures of Chapter 5, Li_2TiO_3

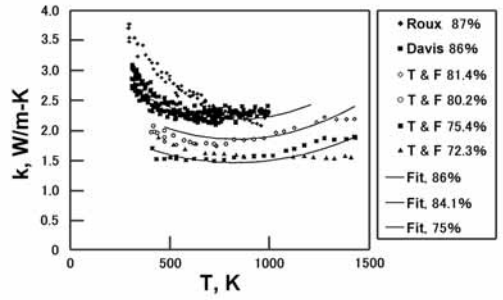

Fig.5.1 Thermal conductivity data for Li_2TiO_3. [27) 28) 92)]

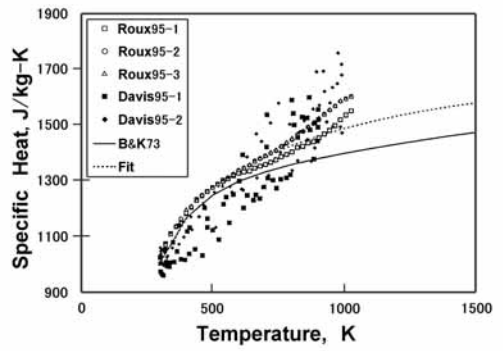

Fig.5.2 Specific heat data for Li_2TiO_3. [28)]

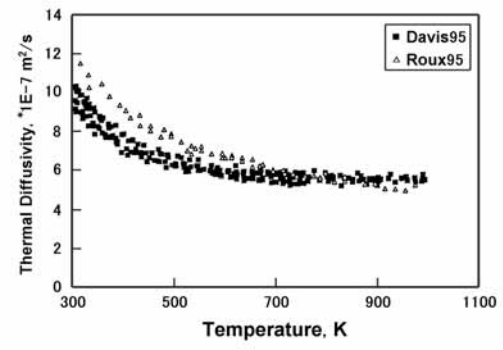

Fig.5.3 Measured thermal diffusivity for 80%TD Li_2TiO_3. The values for each group are an overlay of two or three separate runs. [92) 28)]

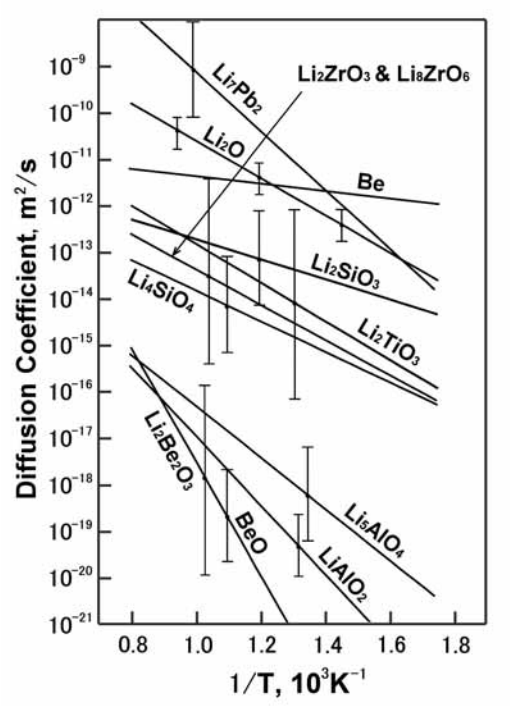

Fig.5.5 Summary of tritium diffusion coefficient in Li_2O, Li_2ZrO_3, Li_2TiO_3 and Li_4SiO_4. [18)]

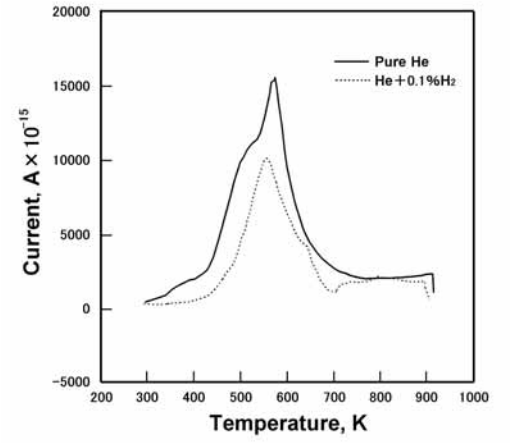

Fig.5.7 Effect of purge gas composition on tritium release from sample sintered at 1498 K and heating rate of 2K/min. (Li_2TiO_3). [2) 67)]

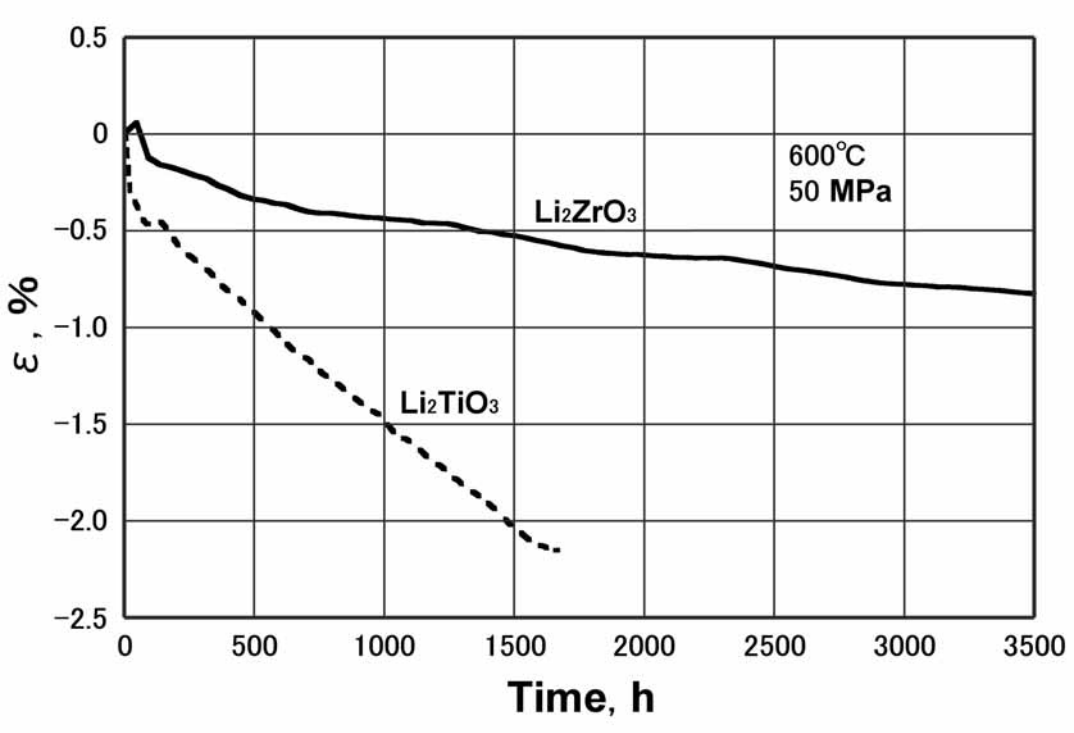

Fig.5.4 Thermal creep rate of Li_2TiO_3 at 600℃ and 50 MPa. [92]

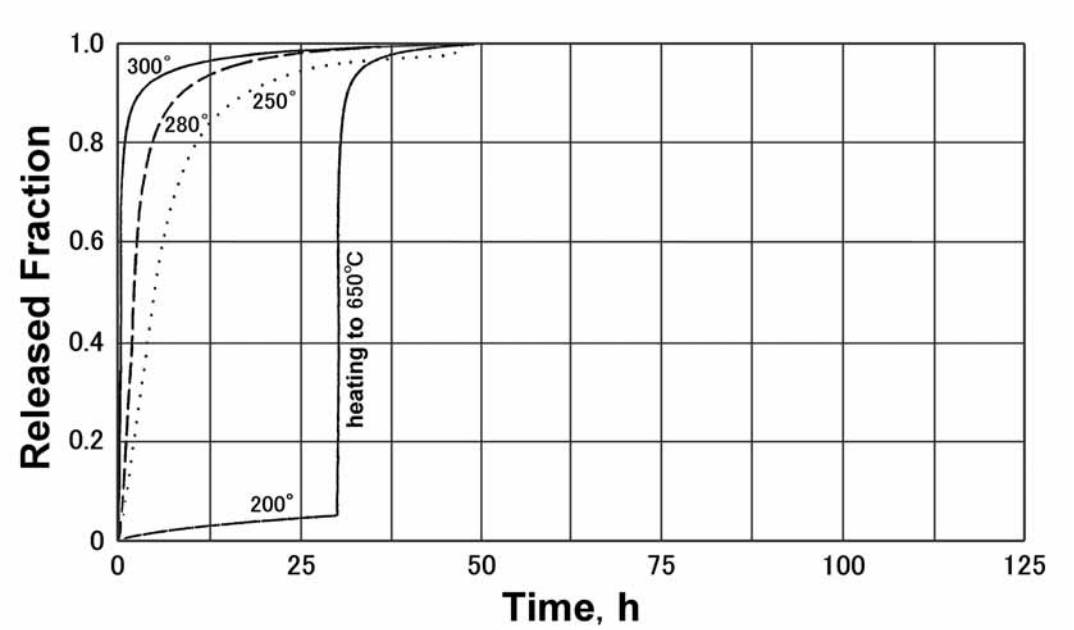

Fig.5.6 Isothermal tritium release at 300℃, 280℃, 250℃, 200℃, in He+0.1%H_2 purge gas, flow rate 2.4lh^{-1} for Li_2TiO_3. [2) 50) 51)]

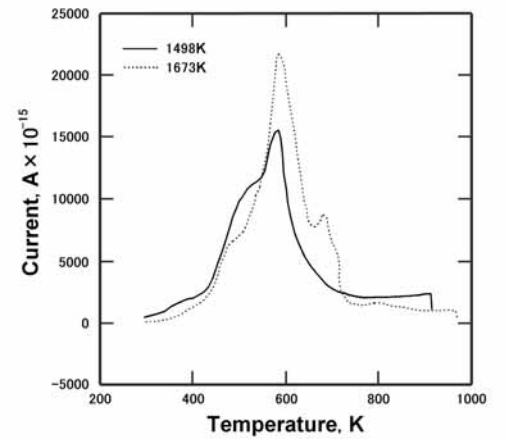

Fig.5.8 Effect of sintered temperature on tritium release for a purge gas of pure helium and heating rate of 2K/min. (Li_2TiO_3). [2) 67)]

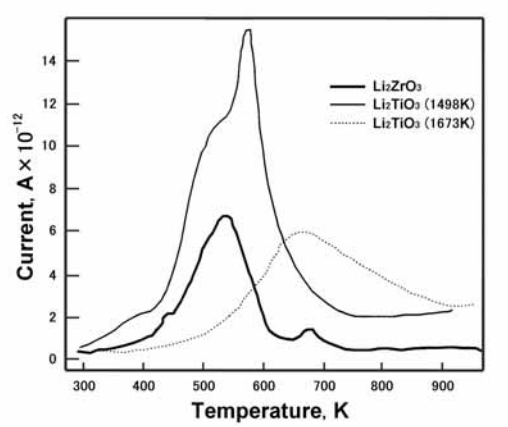

Fig.5.9 Tritium desorption curves for Li_2ZrO_3 and Li_2TiO_3 at a linear heating rate of 2K/min., pure He sweep gas. [2) 67)]

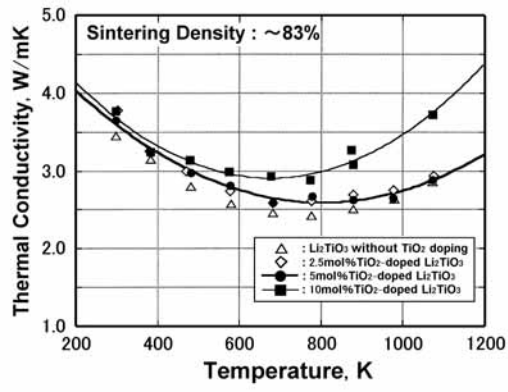

Fig.5.10 Temperature dependency of thermal conductivity for TiO_2 doped Li_2TiO_3 pellets. [93)]